

## Towards coherent control of supersonic beams: a new approach to atom optics

This article has been downloaded from IOPscience. Please scroll down to see the full text article.

2006 New J. Phys. 8 77

(<http://iopscience.iop.org/1367-2630/8/5/077>)

View [the table of contents for this issue](#), or go to the [journal homepage](#) for more

### Download details:

IP Address: 131.152.109.129

The article was downloaded on 09/01/2011 at 16:48

Please note that [terms and conditions apply](#).

## Towards coherent control of supersonic beams: a new approach to atom optics

A Libson<sup>1</sup>, M Riedel<sup>1</sup>, G Bronshtein<sup>2</sup>, E Narevicius<sup>1</sup>,  
U Even<sup>2</sup> and M G Raizen<sup>1</sup>

<sup>1</sup> Center for Nonlinear Dynamics and Department of Physics,  
The University of Texas at Austin, Austin, TX 78712-1081, USA

<sup>2</sup> Sackler School of Chemistry, Tel-Aviv University, Tel-Aviv, Israel  
E-mail: [raizen@physics.utexas.edu](mailto:raizen@physics.utexas.edu)

*New Journal of Physics* **8** (2006) 77

Received 24 April 2006

Published 29 May 2006

Online at <http://www.njp.org/>

doi:10.1088/1367-2630/8/5/077

**Abstract.** A supersonic beam of noble gas atoms is a source of unprecedented brightness. A novel short pulse supersonic nozzle is developed with beam intensity that is higher by at least an order of magnitude than other available sources. We show how this beam can be coherently slowed and focused using elastic reflection from single crystals. Simulations show beam fluxes of  $10^{11}$  atoms  $s^{-1}$  at velocities of  $50 \text{ m s}^{-1}$  and temperatures of less than  $20 \mu\text{K}$  in the longitudinal direction. Possible applications of this slow beam to the study of atom-surface interactions and atom interferometry are discussed.

**Contents**

<b>1. Introduction</b>	<b>2</b>
<b>2. High intensity cryogenic pulsed supersonic nozzle</b>	<b>3</b>
<b>3. Slow atom source: a single-crystal beam slower</b>	<b>5</b>
<b>4. Atomic mirrors and lenses</b>	<b>6</b>
<b>5. Velocity dispersion compensation piston</b>	<b>7</b>
<b>6. Atom beam splitter</b>	<b>7</b>
<b>7. Noble gas atom detector</b>	<b>8</b>
<b>8. Simulation of the beam</b>	<b>8</b>
<b>9. Proposed uses of the beam</b>	<b>11</b>
<b>10. Conclusion</b>	<b>13</b>
<b>Acknowledgments</b>	<b>13</b>
<b>References</b>	<b>13</b>

**1. Introduction**

Atom optics has been a rapidly growing field in recent years due to the enormous potential for precision measurements as well as for fundamental physics [1]. The main focus to date has been on methods of laser cooling and trapping to control atomic translational motion, combined with the control of the internal atomic state. An alternative approach has been to develop atom optics tools that are species independent such as transmission diffraction gratings and transmission Fresnel lenses [2, 3]. Atom optics with ground-state noble gases such as helium and neon has been limited to the latter approach due to the lack of accessible optical transitions. This fact makes control and detection problematic and thus work with these atoms has been much more limited. Nevertheless, ground-state noble gas atoms have two remarkable properties that make them ideal for atom optics and interferometry. First, very high intensity noble gas supersonic beams are readily available [4]. Secondly, atomically flat single-crystal surfaces such as Si and LiF reflect these atoms with high probabilities [5]. In addition, single-crystal surfaces have well-defined periodic structures and can also be used as diffraction gratings for atomic beams.

Atomic beams are traditionally created by allowing gas to escape from a source with a small aperture and collimating the output. In the dilute-gas regime, where the mean free path is larger than the aperture size, the resulting beam has a very broad distribution in velocity as well as angle. As the pressure is increased in the source, the resulting beam becomes very monochromatic and directional, a property of supersonic expansion [4]. To reach the required pressures of several atmospheres, noble gases are typically used as the primary gas and they are ‘seeded’ with another gas which is carried along. The best performance is obtained for a pure supersonic beam of helium where the highest pressure is possible.

The elastic scattering probability of a noble gas impinging on a single crystal surface is well described by the Debye–Waller factor and decreases exponentially with increasing incident energy [6]. Large improvements in reflection probability can thus be obtained by lowering the velocity of the atoms.

It is proposed to combine these two features to slow a supersonic beam of ground-state helium by elastic reflection from a moving single crystal mounted on a spinning rotor.

Doak *et al* [7] suggested a similar experiment; however, the estimated slow beam flux was only  $6 \times 10^5$  atoms  $s^{-1}$ . We were able to increase the expected beam flux to  $10^{11}$  atoms  $s^{-1}$  by using atom focusing and near normal reflection from the receding crystal. Moreover, a supersonic nozzle that is able to achieve atom beam intensities as high as  $4 \times 10^{23}$  atoms  $s^{-1} sr^{-1}$  has been developed.

To the best of our knowledge, Gupta and Herschbach demonstrated the only experimental realization of supersonic beam slowing by mounting the supersonic nozzle on a spinning rotor [8]. However, their continuously operating room temperature nozzle created a high background gas pressure that attenuated the slow beam by scattering and limited the final translational velocity of a  $10^{12}$  atom  $s^{-1}$  xenon beam to  $70$  m  $s^{-1}$  having a transverse temperature of several kelvin.

In section 2, design details and experimental results of pulsed cryogenic supersonic nozzle are presented. In sections 3–7, a set of atom optics elements that include a slow atom source, focusing mirror and single-crystal beam splitter is proposed. Beam simulation results are given in section 8, and possible applications for the slowed beam in section 9.

## 2. High intensity cryogenic pulsed supersonic nozzle

Our supersonic nozzle research was driven by a need for a pulsed atomic beam source with the highest possible intensity and reduced velocity in the lab frame with a narrow distribution of velocities. As will be evident shortly, not all these beam properties can be fulfilled simultaneously. To test this concept, the electromagnetic actuated pulsed valve [9, 10] and vacuum system have been modified. There are several modifications involved.

- (i) The magnetic circuit efficiency of the valve mechanism is increased, reducing the heat dissipation so that we could attach the valve to a temperature-controlled cold finger cryostat. We use ‘Permendur’ alloy with high saturation field at the critical parts of the magnetic circuit. The increased magnetic field and limited travel of the plunger (0.05 mm) allowed us to reduce the heating by an order of magnitude (to 3 mJ per pulse). Extensive computer simulation of the magnetic fields and forces that are generated in the highly saturated magnetic parts allowed us to optimize the geometry [11]. The valve opening time was  $10 \mu s$  at pressure of 100 bars. During this period, the valve releases about  $3 \times 10^{16}$  helium atoms (about  $1 \text{ mm}^3$  at normal temperature and pressure).
- (ii) The conical nozzle is replaced with a trumpet shaped nozzle (0.2 mm inlet diameter, 3 mm length and exit diameter of 2 mm). The trumpet nozzle generated a very narrow beam ( $16^\circ$  FWHM) and avoided reflected shock waves inside the nozzle that were found in flow simulations of simple conical nozzles [12, 13]. The narrow beam together with the high pressure and large nozzle diameter generated an intense flux of helium. At the peak of the pulse, the beam brightness is  $4 \times 10^{23}$  atoms  $s^{-1} sr^{-1}$ . Such a high beam flux was generated at a modest requirement of vacuum pumping speed ( $300 \text{ l s}^{-1}$ ) due to the short pulse time, and will allow us to operate at ultra high vacuum (UHV) conditions to perform surface scattering after one additional stage of differential pumping. This beam intensity is much higher than that generated by other sources [14]–[16] (by at least an order of magnitude). The pumping requirements are reduced by at least two orders of magnitude compared to cw sources. It is true that the duty cycle of this mode of operation is much smaller than

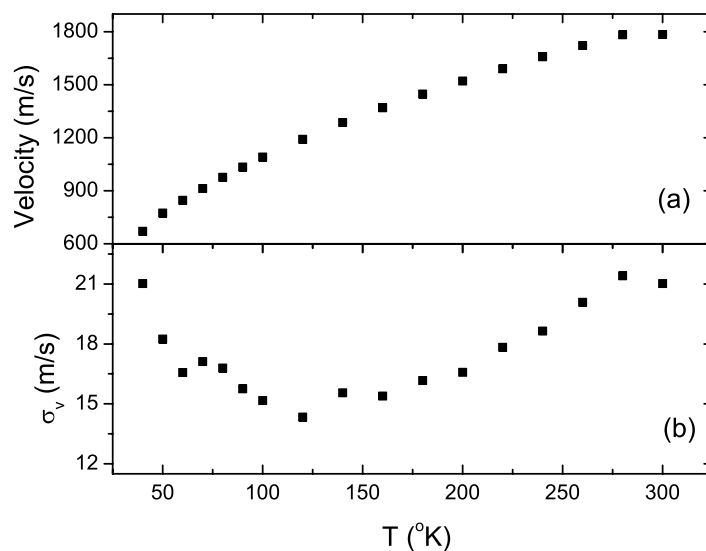


**Figure 1.** Velocity of a helium jet as a function of source temperature (a), the standard deviation of the velocity distribution as a function of source temperature (b).

cw nozzles, however, our beam slower is pulsed as well and is thus better matched to a pulsed-beam source.

- (iii) The beam was skimmed by a 4 mm diameter inlet narrow conical skimmer [17]. It is not surprising that the higher beam intensity here will require modification to the skimmer shape and position. The skimmer distance from the nozzle was 200 mm as shorter distances caused excessive skimmer interference. The term ‘skimmer interference’ is used to denote reduced beam intensity and higher temperature of the beam due to molecules scattered at the finite skimmer entry surface [18, 19]. We found out by direct simulation Monte Carlo (DSMC) simulation that the stationary boundary layer on the conical skimmer outer surface contributes more to this molecular scattering than the actual geometric sharp entrance surface [20]. The simulations indicated that cooling the skimmer can reduce the energy of the atoms that are scattered into the skimmer. The skimmer was conduction cooled by a copper braid attached to a liquid nitrogen pool type cryostat.
- (iv) A pulsed, coaxial hot filament ionizer was placed immediately after the skimmer to excite a small fraction of the gas pulse and create a neutral meta-stable sheath of helium atoms that can be detected by a microchannel plate (MCP) detector after a 2 m flight. By varying the delay of the short ( $2 \mu\text{s}$  long and focused to 1 mm in space) excitation pulse, it could be determined that the gas pulse width was  $20 \mu\text{s}$  at the ionizer position. Only the central (coldest) part of this gas pulse was excited to measure its time spread as this packet travelled down the flight tube to the detector. By measuring the total flight time ( $\sim 1$  ms) and the width of the arriving gas pulse ( $\sim 10 \mu\text{s}$ ) the velocity distribution parameters could be determined. The results are displayed in figures 1(a) and (b). The velocity drops as expected with the source temperature. The velocity spread does not change as much as the velocity itself. It drops from  $\sim 22 \text{ m s}^{-1}$  to a broad minimum of  $\sim 15 \text{ m s}^{-1}$ , and rises again below 100 K. This rise is attributed to the formation of helium clusters in the beam, releasing their condensation

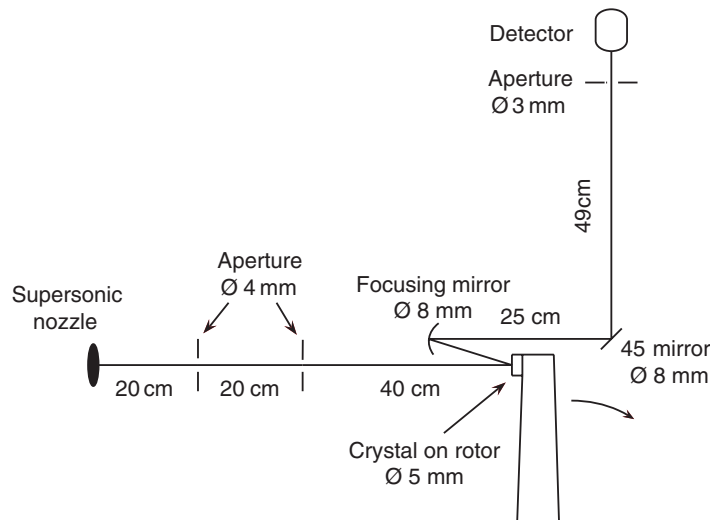


**Figure 2.** Schematic drawing of the proposed beam slower apparatus. The atomic beam is collimated by two apertures. It is then slowed by reflection from the moving rotor, focused by a curved mirror and finally deflected by a second mirror into the detector.

energy and preventing further cooling. The requirement of having both high intensity beams and low velocity spread are difficult to achieve together. Condensation can start easily in an intense beam where three-body collisions are not rare. It is a surprise that the velocity spread does not change much, and we plan to look into this phenomenon further, using other gases and gas mixtures. It is possible though, as shown here, to generate a helium beam of high intensity, moving with a velocity of about  $900 \text{ m s}^{-1}$ , and a standard deviation of the velocity distribution of only  $16 \text{ m s}^{-1}$ .

### 3. Slow atom source: a single-crystal beam slower

Similar to the beam paddle that was developed for neutrons [21], we intend to reduce the mean velocity of the supersonic beam by specularly reflecting the atoms from a single-crystal Si(111) surface which moves along the beam direction. For a linearly moving mirror, the speed of the atoms after hitting the mirror will be  $v_a - 2v_m = v_f$ , where  $v_a$  is the initial velocity of the atoms,  $v_m$  is the velocity of the mirror and  $v_f$  is the final velocity of the atoms. In order to slow the supersonic jet of  $v_a = 900 \pm 16 \text{ m s}^{-1}$  helium atoms to a final velocity of  $v_f = 50 \text{ m s}^{-1}$ , the speed of the reflecting surface has to be  $\frac{1}{2}(v_a - v_f) = 425 \text{ m s}^{-1}$ . Clearly the ideal setup would be a mirror that moves linearly in the same direction as the atoms, but it is difficult to repeatedly move a mirror linearly at such high speeds.

Such velocities are, however, readily achievable by mounting the reflecting mirror on the tip of a spinning rotor. A schematic drawing of a possible rotor based beam slowing apparatus is presented in figure 2. Rotary motion, though, creates an unwanted fanning effect. Due to a finite nozzle opening time the temporal extent of our simulated atomic beam arriving at the spinning mirror is about  $15 \mu\text{s}$ . Over this period of time, the angle of reflecting mirror changes

proportionally to the angular velocity,  $\omega$ , and the reflected atomic beam is spread in the rotation plane. To reduce the fanning effect without changing the mirror speed, the rotor diameter is increased and the angular velocity is decreased. We intend to use a tapered titanium alloy rod, approximately 1 m in length, with holders for single-crystal mirrors at each end for our rotor. To achieve a tip velocity of  $425 \text{ m s}^{-1}$ , the rotor has to spin with an angular velocity of  $\omega = 843.8 \text{ s}^{-1}$  or 8057 rpm. Using finite element analysis, it is estimated that centrifugal forces induce a maximal tensile stress that is 4 times lower than the yield tensile strength for the titanium alloy to be used.

#### 4. Atomic mirrors and lenses

An atom mirror has to be atomically flat over a length scale larger than the atomic beam diameter. Usually, atomically flat surfaces are prepared *in situ* by cleaving single crystals under ultra high vacuum. We cannot use this method to produce atomic mirrors, since the mirrors have to be mounted on the tips of our rotor. Fortunately, hydrogen passivated Si (111) surface, Si(111)- $1 \times 1\text{H}$ , can be easily prepared *ex situ* by wet etching of a Si(111) wafer [22]. That allows us to mount the atom mirrors on the rotor tips at atmospheric pressure. Moreover Buckland and Allison [23] have shown that the helium reflectivity of a hydrogen passivated surface does not change over a period of 6 months in an unbaked chamber with base pressure of  $10^{-8}$  torr. This eliminates the need for active *in situ* surface cleaning by argon-ion bombardment or laser pulse desorption of stuck particles [24].

It is important to estimate the fraction of atoms that will be elastically scattered from the atomic mirror. For single-crystal surfaces, the fraction of atoms elastically scattered is given by the Debye–Waller factor [6, 25],

$$\frac{I}{I_0} = e^{-2W}, \quad (1)$$

$$2W = 24mE_{\perp}T_s/(Mk_B\theta_s^2), \quad (2)$$

where  $m$  is the mass of the impinging atom,  $M$  is the mass of the atom in the crystal,  $T_s$  is the temperature of the crystal,  $E_{\perp}$  is the normal incident energy, and  $\theta_s$  is the crystal Debye temperature [25]. For helium atoms coming from a room temperature supersonic nozzle ( $v_a = 1830 \text{ m s}^{-1}$ ) scattered off of a Si (111) surface (kept at room temperature,  $\theta_s = 690 \text{ K}$ ) at  $45^\circ$  incidence the estimated reflectivity is 37.7%. The specular reflectivity is lowered by impurities, steps or etch pits on the surface and by the distribution of the beam intensity over about 40 open diffraction channels. Thus it is not surprising that the experimental specular reflectivity is below 10% under these conditions [26]. Higher reflectivity is expected in our experiment since the relative velocity of helium atoms reflecting from the receding crystal is more than three times smaller. The Debye–Waller factor at this speed ( $425 \text{ m s}^{-1}$ ) is 0.9 and only the 6 first-order diffraction channels remain open.

Slow beam (velocities below  $300 \text{ m s}^{-1}$ ) reflection probabilities are well above 90% and no diffraction channels are allowed. However, at these low velocities quantum effects become important and the exact value of the reflectivity is still an open question.

The inherent divergence of the supersonic beam leads to the loss of useful flux. The rotor fanning effect contributes further to the loss of flux by spreading the beam in the rotation plane.

However, the detrimental effects of beam divergence and fanning can be mitigated by focusing the atomic beam using reflection from a curved mirror surface. The focal length of the focusing mirror has to be close to the distance between the tip of the rotor and the mirror itself (see figure 2). This distance should be minimized to increase the number of atoms hitting the focus mirror after reflection from the rotor. Practical considerations limit the rotor tip to focusing mirror distance to 16 cm in this design.

Doak *et al* [3] have shown helium beam focusing using Fresnel zone plates; however, due to microfabrication resolution limitations, the zone plate diameter was only 0.27 mm. Holst and Allison [27] have demonstrated helium beam focusing using a thin Si wafer bent electrostatically. The minimal focal length achieved using this method is too long for our purposes. Therefore, a fixed focal length design will be used where the silicon wafer is mechanically clamped between two round rings with angled faces. The first experimental results show that a focal length as small as 17 cm can be achieved before breaking a 225  $\mu\text{m}$  thick wafer.

## 5. Velocity dispersion compensation piston

Our method of slowing lowers the beam's degree of monochromaticity because it does not change the standard deviation in translational velocity. This effect can be compensated by taking advantage of almost perfect correlations between the velocity and the position of the atoms in the slow beam. Due to the short opening time of the nozzle and relatively slow propagation velocity, atoms with different velocities are spatially separated by the time of flight. The relationship between the velocity of an atom and its relative position in the beam can be used to compress the velocity of the atom pulse by reflecting the atoms from an accelerating mirror. Assume that the fastest atoms, which arrive at the mirror first, are reflected without having their velocity changed. The slower atoms will be given a kick in velocity upon reflection from the accelerating mirror. Thus, if a suitable acceleration is found, the correlation between an atom's longitudinal position in the beam and its velocity will allow us to accelerate each of the slower atoms up to the speed of the fastest atoms, thereby increasing the atomic beam degree of monochromaticity.

In this system, a simulated  $49 \pm 3 \text{ m s}^{-1}$  atomic beam can be compressed to  $55.3 \pm 0.2 \text{ m s}^{-1}$  given a mirror that can be accelerated to about 60 g. One method of achieving such an acceleration is to mount the mirror on the projectile of a coil gun. A schematic drawing of a possible realization is presented in figure 3. Using this acceleration method, the acceleration of the mirror can be controlled by simply tuning the current in the coils. Coil guns capable of 5000 g accelerations [28] lead us to believe that an experimental realization of such a system is feasible.

## 6. Atom beam splitter

In previous atom optical systems, beam splitting has been accomplished by diffraction from microfabricated transmission gratings [2], diffraction from standing waves of light [29], and by momentum transfer due to atomic transitions [30]. In each of these systems, it is difficult to obtain large opening angles. For the diffraction based beam splitters, the opening angle is determined by the ratio of the de Broglie wavelength of the atoms in the beam to the period of the grating used. By tuning the final velocity of the slow beam, atom de Broglie wavelengths can be achieved in the range of 1–10 Å. A grating period on the order of the de Broglie wavelength

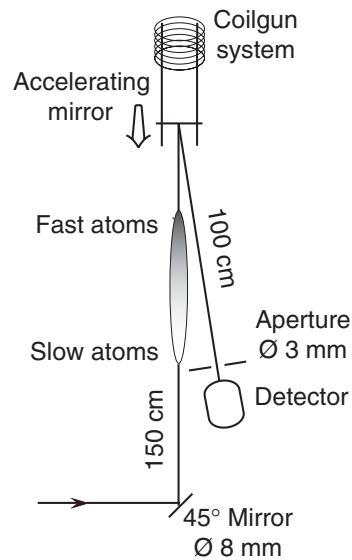


**Figure 3.** Schematic drawing of the proposed velocity compression piston. The atomic beam collides with an accelerating mirror which makes the beam more monochromatic. The mirror is accelerated by a coil gun setup.

would provide large opening angles and it is believed that such a grating could be constructed from a single-crystal surface. Utilizing the periodic structure of a crystalline lattice to create a reflection grating would give a grating period of the appropriate size, yielding the desired opening angles. By controlling the velocity and incident angle of the atoms, it should be possible to restrict diffraction to only a few open channels. As such, the flux in any one channel should be greatly enhanced. Furthermore, by tuning the incoming atom beam energy to match the energy of a selective adsorption resonance, it could be possible to enhance the atom flux into particular diffraction order associated with that resonant state.

## 7. Noble gas atom detector

Detection of the atoms is a crucial step since the high flux would be wasted if it could not be detected. It is planned to use a modified quadrupole mass analyser for the detection of the atoms. The detection efficiency of such a device for room temperature helium is on the order of  $10^{-5}$  [31]. The large volume coaxial ionizer [32] helps to increase the electron emission current and ionization probability can be raised to  $10^{-4}$ . Since the ionization probability scales linearly with the transit time through the ionizer, it is expected that our detection efficiency will be better by about an order of magnitude.

## 8. Simulation of the beam

Monte Carlo method is used to simulate the beam slowing and focusing process. Each run starts with 200 million atoms having Gaussian velocity distribution of  $32 \text{ m s}^{-1}$  FWHM centred around

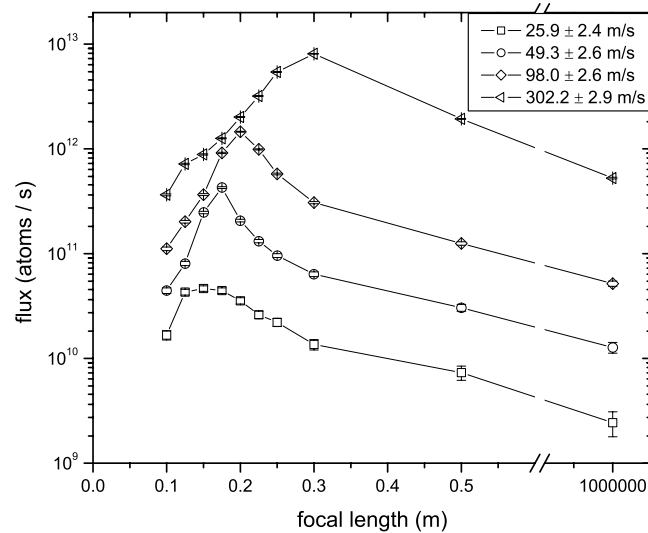


**Figure 4.** Atom flux after passing through the final aperture as a function of focal length for different slowed beam speeds. Flux gains of more than one order of magnitude from focusing are observed.

$900 \text{ m s}^{-1}$  in the propagation direction. The velocity distribution in both transverse directions is  $110 \text{ m s}^{-1}$  FWHM centred at zero. Our simulations only included atoms within two standard deviations of the mean for both the transverse and longitudinal velocity distributions. The final flux is normalized to the expected output flux of the supersonic nozzle,  $\Phi = 1.2 \times 10^{18} \text{ atoms s}^{-1}$ .

Now the beam path of the proposed design is outlined. First, the atomic beam is created at the location of the supersonic nozzle over a period of  $10 \mu\text{s}$ . The beam is then collimated by two 4 mm apertures spaced 20 cm apart (see figure 2). The collimated beam is slowed by a collision with the receding 5 mm diameter crystal located 40 cm away from the last collimating aperture. The slowed beam is focused by an 8 mm diameter concave mirror and is directed to the final 3 mm aperture by a flat 8 mm diameter mirror rotated by  $45^\circ$  with respect to the propagation direction. The distance between the final aperture and the rotor-mounted mirror is 1 m. The reflection probability of the atomic mirrors used in our simulations is given by the Debye–Waller factor.

The simulated beam flux as a function of slow beam velocity and mirror focal length is presented in figure 4. Simulation results show that the flux through the final aperture decreases with final beam velocity. To achieve a slower beam velocity, the rotor has to move faster and the fanning effect increases the spread in the rotation plane. Consequently, more atoms miss the focusing mirror and the flux decreases. It should be noted though that even for the lowest simulated speed of  $25 \text{ m s}^{-1}$ , the flux is well above  $10^{10} \text{ atoms s}^{-1}$  when using the optimal focal length of the atomic lens.

For all final beam velocities, the focusing of the beam increases the flux by more than one order of magnitude. The optimal focal length depends on the speed and increases from 15 cm at  $25 \text{ m s}^{-1}$  to 30 cm at  $302 \text{ m s}^{-1}$ . To illustrate the focusing effect the transverse position distributions of a  $49 \text{ m s}^{-1}$  beam at the plane of the final 3 mm aperture is presented. Figure 5(a) shows the position distribution for an infinite focal length mirror (flat mirror), whereas figure 5(b)

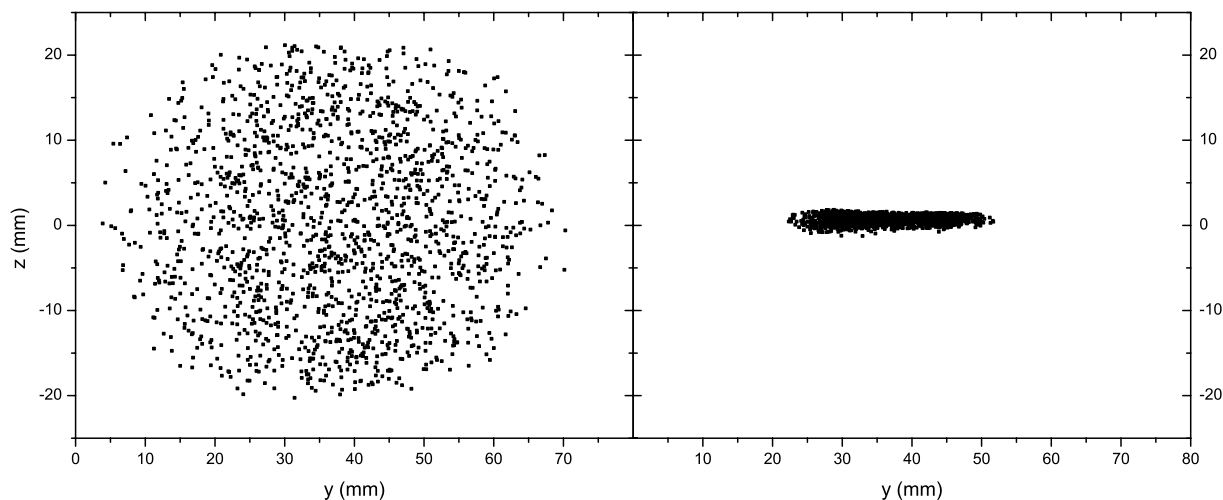


**Figure 5.** Spacial distribution of atoms at the location of the final aperture. Simulated slow beam velocity is  $49 \text{ m s}^{-1}$  in both cases. (a) Infinitely long focal length (standard deviation of 10.35 cm in the  $z$ -direction and 13.5 cm in the  $y$ -direction). (b) Focal length of 17.5 cm (standard deviation of 0.49 cm in the  $z$ -direction and 6.3 cm in the  $y$ -direction).

shows the distribution for the optimal focal length of 17.5 cm. Comparing the standard deviations of the distributions, it can be seen that the mirror indeed reduces the fanning effect (the spread of the atoms in plane of the rotor) by a factor of two. The increase in flux however, results mainly from the focusing in the  $z$ -direction, which reduces the spread in  $z$  by a factor of 20. The reason that the beam cannot be focused as well in the plane of the rotor, is that the fanning effect makes the rotor appear as a source of finite extent in the rotor plane.

A closer examination of the velocity distribution of the slowed beam reveals a useful correlation between the speed and the arrival time of an atom at a specific point in space. In figure 6, the longitudinal velocity of each atom is plotted against the time that has passed from the opening of the nozzle to its arrival at the aperture. The fastest atoms arrive more than 5 ms earlier than the slowest and there is a very strong correlation between time and velocity. An analysis of this correlation shows that by measuring the arrival time with microsecond resolution, the velocity resolution is greater than  $10 \text{ cm s}^{-1}$  which corresponds to an energy resolution of about  $1.5 \mu\text{eV}$ .

Finally, it is shown that the velocity distribution can be compressed by reflection from an accelerated piston. This is only possible because of the high correlation between the arrival time of an atom and its velocity, which is shown in figure 6. In figure 7(a), the longitudinal velocity distribution of the  $49 \text{ m s}^{-1}$  beam is shown as it passes through the final 3 mm aperture. Figure 7(b) shows that the velocity can be compressed by a linearly accelerating piston so that the standard deviation in velocity is  $0.18 \text{ m s}^{-1}$ . Here, the piston is nearly 1.5 m from the  $45^\circ$  mirror and the measurement is taken after a 3 mm aperture which is located 1 m away from the piston. From a statistical analysis of this distribution, it is seen that the longitudinal temperature of this velocity compressed beam is about  $16 \mu\text{K}$ .

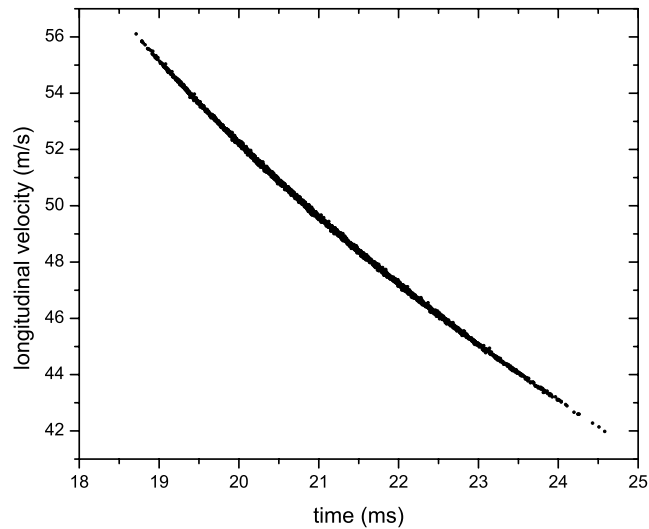


**Figure 6.** Correlation between the velocity and arrival time after passing through the final 3 mm aperture.

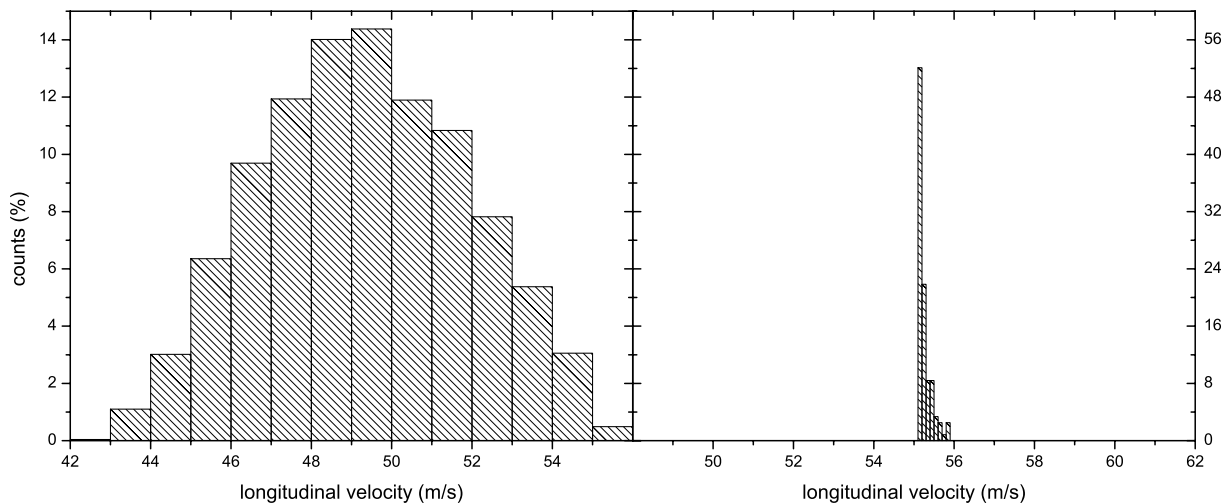


**Figure 7.** Velocity distribution for (a) the uncompressed beam. The mean velocity is  $49.3 \text{ m s}^{-1}$  and standard deviation is  $2.6 \text{ m s}^{-1}$ . (b) The beam compressed with an accelerated piston. The mean velocity is  $55.3 \text{ m s}^{-1}$  and the standard deviation is  $0.18 \text{ m s}^{-1}$ .

## 9. Proposed uses of the beam

A high flux, cold, low energy atom beam is well suited to several experimental applications. In particular, the beam we propose to create would work well for studies of atom–surface interactions and atom interferometry.

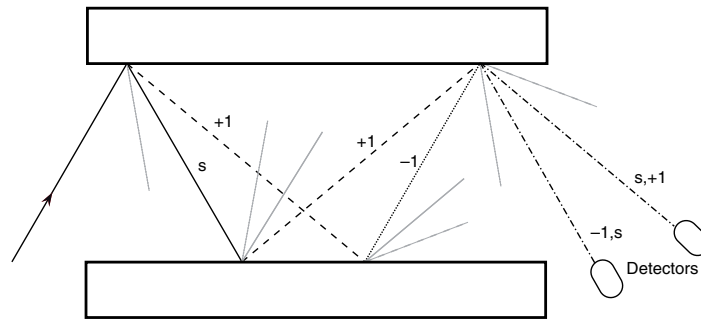


**Figure 8.** Schematic drawing of the proposed single-crystal atomic interferometer. Specular reflected beams are labelled with an  $s$ , diffracted beams with the diffraction order.

One way to better characterize the atom–surface potential would be to study the reflected intensity of an atom beam at different incident energies. Certain incident energies would couple with the bound resonant states of the atom–surface potential through diffraction channels. By measuring the incident energies that couple to these resonant states, one could determine the energy level structure, and thus the precise shape, of the atom–surface potential. There are two reasons why the proposed beam would work so well for these studies. First, the energy resolution of  $1.5 \mu\text{eV}$  as described in figure 6 would give us a much greater resolution than a standard supersonic beam. Secondly, the slow and tunable velocity of our atoms would allow us to study lower energy regimes than have previously been accessible. Finally, a precise measurement of the diffracted angle at a known velocity would provide an independent means by which to measure the lattice constant.

The predicted slow beam would provide many advantages when used for atom interferometric purposes. Ground state noble gases are insensitive to magnetic fields to first order, and due to their low polarizability, they are approximately 100 times less sensitive to stray electric fields than the alkali atoms. For a white light geometry Mach-Zehnder interferometer with length  $L$ , rotating at a rate  $\Omega$  around an axis perpendicular to its plane, the phase shift is  $\varphi = 2\pi\Omega L^2/vd$ , where  $d$  is the grating spacing and,  $v$  is the velocity of the atoms [33]. Thus the sensitivity is inversely proportional to the velocity, favouring a slow beam. The phase shift for an acceleration  $a$  transverse to the direction of atomic motion is  $\varphi = 2\pi aL^2/v^2d$  [33]. Here, the phase shift is inversely proportional to the square of the velocity of the atoms. Since for many applications, the sensitivity will be shot noise limited, the signal to noise ratio will scale with the inverse square root of the number of atoms detected per unit time. For this reason, a high flux beam, such as our simulated beam, will give better counting statistics and thus a higher signal to noise ratio.

The relative phase shift of the atoms in the interferometer is inversely proportional to the grating spacing distance. As such, another method for increasing the sensitivity of the interferometer is to reduce the grating period. The single-crystal reflection grating could provide a means for doing this. In particular, one could construct an atomic interferometer from a single crystal which would be an atomic analogue to the perfect single-crystal neutron interferometer [21, 33]. A schematic of a possible implementation of this can be seen in figure 8. With neutron interferometry the crystal acts as a transmission grating, while in our atomic analogue, crystal surface would act as a reflection grating. The advantages of this design are a large enclosed area,

yielding increased sensitivity, high flux since diffraction is limited to only a few channels, and ease of alignment due to the monolithic design.

## 10. Conclusion

In summary, experimental results from a new supersonic nozzle design are presented and an experiment to slow a supersonic beam of ground-state helium and neon by elastic reflection from a moving single crystal mounted on a spinning rotor is proposed. Design parameters are numerically optimized and it is shown that it should be possible to create beams with speeds as low as  $25 \text{ m s}^{-1}$  that have fluxes of over  $10^{10} \text{ atoms s}^{-1}$ . The beam velocity could be continuously scanned and we should be able to use the correlation between arrival time and velocity to obtain very high energy resolution. We intend to use the slow beam to study atom–surface interaction at previously unavailable energy range and resolution. We also discuss the advantages of using the slow atom beam to construct an atom interferometer.

## Acknowledgments

MGR acknowledges support from the Army Research Office, the National Science Foundation Focus Center, and the R A Welch Foundation. UE acknowledges support from The Israeli Science Fund and The James Franck Foundation.

## References

- [1] Berman P (ed) 1997 *Atom Interferometry* (San Diego, CA: Academic)
- [2] Chapman M S, Ekstrom C R, Hammond T D, Rubenstein R A, Schmiedmayer J, Wehinger S and Pritchard D E 1995 *Phys. Rev. Lett.* **74** 4783
- [3] Doak R B, Grisenti R E, Rehbein S, Schmahl G, Toennies J P and Wöll Ch 1999 *Phys. Rev. Lett.* **83** 4229
- [4] Campargue R (ed) 2001 *Atom and Molecular Beams: The State of the Art 2000* (Berlin: Springer)
- [5] Farías D and Rieder K H 1998 *Rep. Prog. Phys.* **61** 1575
- [6] Burke K and Kohn W 1991 *Phys. Rev. B* **43** 2477
- [7] Doak R B, Kevern K, Chizmeshya A, David R and Comsa G 1997 *SPIE* **2995** 146
- [8] Gupta M and Herschbach D 2001 *J. Phys. Chem.* **105** 1626
- [9] Even U, Jortner J, Noy D and Lavie N 2000 *J. Chem. Phys.* **112** 8068
- [10] Even U, Hillenkamp M and Keinan S 2003 *J. Chem. Phys.* **118** 8699
- [11] Integrated-Engineering-Software 2005 (<http://www.integratedsoft.com>)
- [12] Bird G 2003 DSMC program (G.A.B. Consulting, <http://gab.com.au>)
- [13] Wu J-S, Chou S-Y, Lee U-M, Shao Y-L and Lian Y-Y 2005 *J. Fluids Eng.* **127** 1161
- [14] Campargue R 1984 *J. Phys. Chem.* **88** 4466
- [15] Pedemonte L and Bracco G 2003 *J. Chem. Phys.* **119** 1433
- [16] Schollkopf W and Toennies J P 1996 *J. Chem. Phys.* **104** 1155
- [17] Beam-Dynamics (<http://www.beamdynamicsinc.com>) Skimmer 50.8
- [18] Miller D R 1988 *Atomic and Molecular Beam Methods* vol 1, ed G Scoles (Oxford: Oxford University Press)
- [19] Beijerinck H C W, Van Gerwen R J F, Kerstel E R T, Martens J F M, Van Vliembergen E J W, Smits M R T and Kaashoek G H 1985 *Chem. Phys.* **96** 153
- [20] Jordan D C, Barling R and Doak R B 1999 *Rev. Sci. Instrum.* **70** 1640
- [21] Bonse U and Rauch H (ed) 1979 *Neutron Interferometry* (Oxford: Oxford Science Publications)
- [22] Dumas P, Chabal Y J and Higashi G S 1990 *J. Electron Spectrosc. Relat. Phenom.* **54/55** 103

- [23] Buckland J R and Allison W 2000 *J. Chem. Phys.* **112** 970
- [24] Althoff F, Andersson T and Andersson S 1997 *Phys. Rev. Lett.* **79** 4429
- [25] Manson J R 1991 *Phys. Rev. B* **43** 6924
- [26] MacLaren D 2005 private communication
- [27] Holst B and Allison W 1997 *Nature (London)* **390** 244
- [28] Kaye R J, Cnare E C, Cowan M, Duggin B W, Lipinski R J, Marder B M, Douglas G M and Shimp K J 1993 *IEEE Trans. Magn.* **29** 680
- [29] Giltner D M, McGowan R W and Lee S A 1995 *Phys. Rev. Lett.* **75** 2638
- [30] Kasevich M and Chu S 1991 *Phys. Rev. Lett.* **67** 181
- [31] Kuhnke K, Kern K, David R and Comsa G 1994 *Rev. Sci. Instrum.* **65** 3458
- [32] Even U unpublished results
- [33] Clauser J F 1988 *Physica B* **151** 262